Zeitschrift für Geomorphologie, Vol. 62 (2019), Suppl. 2, 101–125 **Article**
Stuttgart, October 2019

Event deposits in the Eastern Thermaikos Gulf and Kassandra Peninsula (Northern Greece): evidence of the 479 BC "Herodotus tsunami"

Margret Mathes-Schmidt, Ioannis Papanikolaou, Klaus Reicherter, Aggelos Pallikarakis

With 6 figures and 5 tables

Abstract. Event deposits of high-energy waves in the Eastern Thermaikos Gulf and Kassandra Peninsula (Northern Greece) are investigated, and evidence for the 479 BC "*Herodotus tsunami*" is described for the first time. One of the first historical descriptions of tsunami waves and its effects on Persian troops near Potidaea in 479 BC was made by Herodotus. Sedimentary traces of tsunamis were investigated in cores from different areas from Angelochori in the north to the ruins of ancient Mende in the south (Kassandra peninsula). Evidence for one, locally two high-energy events, on the coasts of Chalkidiki is found. These layers are preserved in flat and lagoonal areas at least from 100 m of the present-day beach. Within ancient Mende, a high-energy layer was encountered. Besides a vast amount of ceramics, the layer also contains articulated bivalve shells. These were dated to a time span between 712 and 521 cal yrs BC by radiocarbon including a reservoir effect of 400 ± 40 years. Resulting ages resemble the time the tsunami mentioned by Herodotus in 479 BC. Deposits of a further event affecting the Thermaikos Gulf were dated between the 7^{th} to 10^{th} cent. AD.

Key words: northern Greece, extreme wave event, tsunami deposits, 479 BC tsunami

1 *Introduction*

In the winter of 479 BC, during the Persian-Greek war, the Persian army besieged Potidaea city, on the western Chalkidiki peninsula (Kassandra, the ancient Pallene in Greece, Fig. 1). The Herodotus Histories (Urania, Book 8, 129) report an unusual sea withdrawal followed by inundations by several large waves. Many soldiers of the Persian troops perished by drowning and the survivors were killed by the Potideans. The description of this event did not refer to neither a storm (Smid 1970), nor reported association with earthquakes (Ambraseys 2009). Other possible causes for this event could be related with meteorological effects or submarine slumping (Ambraseys 2009); these cannot be ruled out in the studied case. It took more than 2,000 years to interpret Herodotus report as a tsunami, the first historical tsunami ever (Bolt 1978, Smid 1970).

The proximity to the North Anatolian Fault Zone (NAFZ) in the North Aegean Basin offers the possibility of extreme wave events (EWE) induced by seismicity (Reicherter et al. 2010). The westernmost, 55 km long segment of the NAFZ, was taken for the modelling of tsunami sources, which may have affected the Thermaikos Gulf and Chalkidiki peninsula. It can cause earthquakes with possible magnitudes around 7 or more (Papanikolaou & Papanikolaou 2007). Wave heights dependent from coastal morphology may reach more than 2 meters with considerable run-up in flat coastal areas (Reicherter et al. 2010). We present new data from the Kassandra peninsula, the south-western branch of Chalkidiki. We complement this with ra-

DOI: 10.1127/zfg_suppl/2019/0612 0372-8854/19/0612 $ 6.25

diocarbon age of sites of our earlier investigations (Reicherter et al. 2010). The research aims to verify whether a tsunami occurred in 479 BC, to identify and trace candidates of EWE in the Thermaikos Gulf. This contributes to enhance the existing tsunami record for the Northern Aegean and can help to assess the hazard by EWE, specifically tsunamis.

1.1 *Regional settings*

The study area stretches from Angelochori in the north to the ancient Mende in the south along the eastern coast of the Thermaikos Gulf (Greece). We focussed on 6 areas along the coast (Fig. 1A), which may provide archives for EWE deposits. Climate conditions are subtropical with dry, hot summers and mild, wet winters. The main wind directions in summer are from N and NE, so-called Etesians, in April, May and July also winds from S and SE are common (Pyökäri & Lehtovaara 1993). In winter wind reaches up to 8 Beaufort (Pyökäri & Lehtovaara 1993, Poulos et al. 2000, Hofrichter et al. 2002), whereas 3 to 5 Beaufort is considered as average.

The Thermaikos Gulf (Fig. 1A) opens southward from the Thessalonica Bay to the Aegean Sea. At the eastern coast, the sandy spit of Cape Epanomi marks the transition from the inner to the outer Gulf (Poulos et al. 2000). Water depth increases from c. 25 m in the Thessalonica Bay to a maximum of c. 200 m in the Thermaikos Gulf, and then rapidly deepens to more than 1500 m in the Sporades Basin. The coast between Thessalonica and Potidaea has a low relief, flat and narrow beaches with beach ridges mostly not higher than 1 m – 2 m with intercalated higher cliff sections. Cliffs with small, pocket-like beaches, getting steeper towards its southern end, characterize the southern coastline of Kassandra peninsula. The highly inhabited and agriculturally used coast also has low vegetated dunes, more or less silted up lagoons and salines are present (Angelochori, Cape Epanomi). These flat areas are regarded as potential archives for tsunami deposits.

The surface water currents enter the Gulf from the south parallel to the coast and turn anti-clockwise in southward direction parallel to the western coast in general. Variations of this system are seasonal changes in wind directions. The average wave heights depending from wind speed and wind directions are around 0.5 m –0.7 m for the outer shelf. The tidal amplitudes do not exceed 0.1 m (Poulos et al. 2000). For Thessalonica and Cape Epanomi Pavlopoulos et al. (2011) give a mean tidal amplitude of 0.24 m. Along the coast of Chalkidiki the recent shelf sediments mostly consist of fine sand with low mud and silt content (Poulos et al. 2000).

1.2 *Tsunami history of the North Aegean*

The database of Mediterranean paleotsunamis including the Northern Aegean Sea is continuously growing due to the use of a set of different sources like historical documents, geological and geomorphological investigations (Papadopoulos et al. 2014). The North Aegean Sea is classified as region with low tsunami potential (Papadopoulos et al. 2014). This may be due to the long recurrence periods of tsunamis or because of the low to medium height of expected tsunami waves (Reicherter et al. 2010). Tsunami generating events are earthquakes and landslides, which are often triggered by earthquakes or volcanic eruptions (Papadopoulos et al. 2014). Papanikolaou & Papanikolaou (2007) and Reicherter et al. (2010) identified the southern marginal fault of the North Aegean Basin as a possible source of tsunami generating

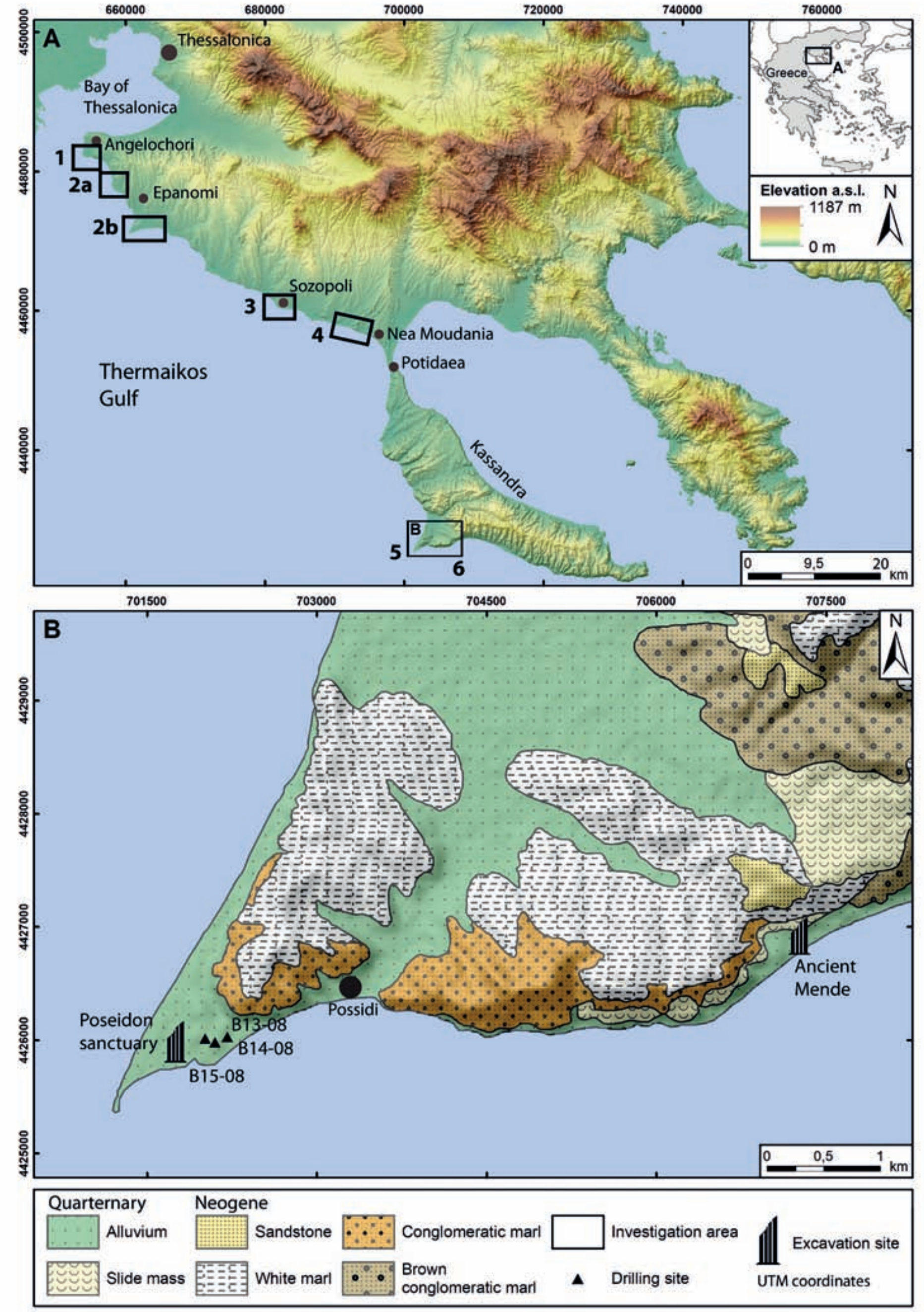

Fig. 1. **A:** Study areas at coast of Chalkidiki, eastern Thermaikos Gulf. Area 1 – Angelochori, area 2a/2b – north/south Cape Epanomi, area 3 – Sozopoli, area 4 – Nea Moudania, Kassandra peninsula: area 5 – Possidi, area 6 – ancient Mende. **B:** Geology of the investigation area on Kassandra based on Guy et al. (1969) and topography on U.S. Geological Survey (2014).

Table 1. Overview of Thermaikos Gulf tsunamis and adjacent areas in the South.

No.	Date	Locality	Cause	Comments	References
1	479 BC	Potidaea	no earthquake or storm reported		1, 2, 4, 8, 5, 12
2	426 BC	Skopelos Island	earthquake		12
3	330 BC	Lemnos Island	earthquake		9
4	1902 July	Thessaloniki	earthquake	flooding of the harbour	2, 3, 5, 7, 12
5	1956 July	Skopelos Island	Earthquake, magnitude > 7 and seismically triggered landslide		2, 5, 11, 12
6	1959 February	Thessaloniki	No earthquake reported	inundation depth of 1 m,	2, 5, 12
7	1962 May	Lemnos Island	Earthquake magnitude 4.5	shallow waves	12
8	1965 March	Skiathos Island	Earthquake magnitude 6.3		12
9	1968 February	Lemnos Island	Earthquake magnitude 7.1	max. water height in harbour of Myrina 1.20 m	7, 9, 10, 12
10	1983 August	Myrina, Lemnos Island	Earthquake magnitude 7	shallow waves at Myrina	4, 5, 9, 12

References: 1: Smid (1970), 2: Papadopoulos & Chalkis (1984), 3: Soloviev (1990), 4: Papazachos & Papazachou (1997), 5: Soloviev et al. (2000), 6: Papadopoulos (2002), 7: Papadopoulos & Fokaefs (2005), 8: Ambraseys (2009), 9: Altinok et al. (2011), 10: Maramai et al. (2014), 11: Necmioglu & Özel 2015, 12: National Geophysical Data Center (2019). Grey background: Tsunami observation in the Thermaikos Gulf; White background: Tsunami observation in southerly adjacent areas.

earthquakes with a magnitude around 7 and a vertical displacement of 3 m – 4 m. Necmioglu & Özel (2015) calculated a maximum wave height for the Northern Aegean Sea < 1 m for earthquake triggered tsunamis. However, the effects of accompanying landslides are not taken into account in these calculations (Necmioglu & Özel 2015).

In the Thermaikos Gulf, the 479 BC event is the oldest accepted tsunami event in history. As cause for this event neither an earthquake nor a storm is mentioned in historical sources (Ambraseys 2009, Smid 1970).

For the Thermaikos Gulf two tsunamis occurred in July 1902 induced by earthquakes (Papadopoulos & Chalkis 1984, Soloviev 1990, Soloviev et al. 2000, Papadopoulos 2002, Papadopoulos & Fokaefs 2005, National Geophysical Data Center (2019) and in February 1959 (Papadopoulos & Chalkis 1984, Soloviev et al. 2000, National Geophysical Data Center (2019), whereof the cause is unknown (Table 1). From the older event the flooding of the harbour of Thessalonica is reported (Soloviev et al. 2000, National Geophysical Data Center 2019), from the younger tsunami in 1959 an inundation depth of 1 m at Thessalonica was described (Soloviev et al. 2000, National Geophysical Data Center 2019).

Several tsunamis (Table 1), caused by earthquakes, near to the Thermaikos Gulf were observed on the island of Lemnos in 330 BC, 1968, 1962 and 1983 (Papazachos & Papazachou

1997, Papadopoulos & Fokaefs 2005, Altinok et al. 2011, Maramai et al. 2014, National Geophysical Data Center 2019). Three further tsunamis triggered by earthquakes were described from Skolepos and Skiathos Islands in 426 BC, 1956 and 1965 (Table 1, Papadopoulos & Chalkis (1984), Soloviev et al. (2000), National Geophysical Data Center (2019)). No data about events before 479 BC are listed in the databases that compile tsunami effects along the Thermaikos Gulf.

2 *Study areas*

2.1 *Drilling locations*

Field work concentrated on areas sheltered from direct wave action such as lagoonal zones and smooth depressions behind beaches. Drillings were situated at 5 sites (Fig. 1A, Table 2): Angelochori (1), Epanomi (North –2a, South –2b), Sozopoli (3) with southward adjacent areas near Nea Moudania (4) and Possidi (5).

The salines and lagoon of Angelochori are located on a sandy spit at the transition of the Thessalonica Bay to the Thermaikos Gulf (Fig. 1A, area 1). Messinian sands form the geological basement of the area (Lalechos & Bizon 1969). Cape Epanomi (Fig. 1A, area 2b) consists of a large spit with vegetated dunes and a central lagoon. It is situated at the transition from the inner to the outer Thermaikos Gulf. This position leads to substantial seasonal changes in wind and wave action in particular resulting in a higher amount of coarse sediments in the southern part (Poulos et al. 2000). In the northern part chevron-like features appear on aerial images, which may be of Aeolian or spill-over origin (Bourgeois & Weiss 2009). Aside from the lagoonal area marine sandstones of Pliocene age with some intercalations of gravels, clayey and calcareous material crop out (Lalechos & Bizon 1969). Close to the village of Sozopoli behind a shallow beach berm a dry lagoonal area besides a dune field is preserved (Fig 1A, area 3). Nearby, Neogene sands of the Miocene to Pliocene (Mollat et al. 1978) form a huge cliff.

Possidi and Mende are situated on Kassandra peninsula (Fig. 1A). The coastal area comprises mainly Neogene sands, conglomerates and marls of terrestrial and marine origin besides alluvium (Fig 1B; Guy et al. 1969).

2.2 *Mende*

Ancient Mende (= mint), 1.5 km south-east of the modern village of Kalandra, was an important city in the classic Hellenistic period, famous for its special wine and silver mining. It was founded as a colony by Eretria in the 9th cent. BC (Ainian & Leventi 2009) but settlement reaches back to the 12th cent. BC. The city and the acropolis were settled on the hill whereas downhill near to the coast public buildings (proasteion) were situated and at the beach a cemetery, dating from the 8th to 4th cent. BC, was excavated where mainly infants were buried. Continuous settling persists from 9th to 4th cent. BC (Tsigarida 2008). After the foundation of Cassandreia in 316 BC on the ruins of ancient Potidaea the inhabitants of Mende were forced to resettle in the new city (Stillwell et al., without year). The excavation lies close to the small sandy coast c. 2–3 m above sea level (Fig 2A). Landwards the north-east the ground rises quickly. The coastal zone is built of alluvium, the hills of Neogene marls, conglomerates and sands (Guy et al. 1969, Fig. 1B).

Table 2. Data and coordinates (UTM) of the drilling places mentioned in this paper. Cores from area 1, 2 and 3 are described in Reicherter et al. (2010). SA: sieve analysis, MS: magnetic susceptibility, M: micropaleontology, RD: radiocarbon dating

Investigation area	**Outcrop ID and coordinates (GPS)**	**Height above sealevel**	**Description of the location**	**Lab examination**
(1) Angelochori	B3-07: 34T 654474.32 4482507.75 B4-07: 34T 654800.21 4482605.19 B5-07: 34T 654930.40 4482802.23 B6-07: 34T 654761.25 4482917.19	c. 0 m – 1 m	dry lagoonal area between a saline and beach ridge, 340 m – 820 m from the coastline	SA, MS, M,
(2a) Cap Epanomi north	B13-07: 34T 658475.21 4477790.05 B14-07: 34T 658465.69 4478039.73	c. 1 m – 1.5 m	c. 300 m landward behind a lagoon	SA, MS, M, RD
(2b) Cap Epanomi south	B12-07: 34T 661822.42 4472441.90 B16-07: 34T 662150.59 4472582.26	c. 1 m	along a small spit, between the beach and a lagoonal area, 800 m to 1000 m behind the coastline	SA, MS, M
(3) Sozopoli	B7-07: 34T 682385.32 4460493.60 B9-07: 34T 682589.08 4460452.26 B20-07: 34T 682765.32 4460376.93	c. 0 m – 1 m	along the coastline c. 90 m – c. 250 m behind the beach ridge	SA, MS, M, RD
(4) Nea Moudania	B17-08: 34T 692213.46 4457616.61 B21-08: 34T 689623.61 4458385.23 B23-08: 34T 691754.83 4457811.54	c. 0 m – 1 m	along the coastline in a flat area behind the beach ridge, distance to the sea: 50 m – 200 m	SA, MS, M
(5) Possidi	B13-08: 34S 702208.00 4426029.00 B14-08: 34S 702099.00 4425983.00 B15-08: 34S 702011.00 4426016.00	c. 0 – 1 m	in a flat area between the Poseidon sanctuary and a small hill (fig. 2B)	SA, MS, M
(6) Mende	34 S 707279.00 4426869.00	excavation ground: c 2 m – 3 m bgl	excavation (fig. 2A), distance to the recent coastline: c. 90 m	RD, M

2.3 *Possidi*

The drilling area lies on a spit reaching into the Thermaikos Gulf close to a small hill built of Miocene marls and conglomerates (Fig. 1B). South-west of the Possidi village and south of the

Fig. 2. A – Excavation of ancient Mende (Fig. 1A, area 6) with sampling sections. B – Drilling site B13-08 northward of the Poseidon sanctuary. In the north-eastern background a small hill built of Miocene marls and conglomerates elevates, to the south-east the sea lies behind a small beach ridge.

drilling site the Poseidon sanctuary is located at the transition to a flat sand cape, which forms the outer part of the spit. The inner part of the cape is covered by sand dunes. The extra-urban sanctuary of Poseidon belongs to Mende and was built in the 10th cent. BC around an ash altar dated to the 12th cent. BC (Moschonissioti 1998, Tiverios 2008). The sanctuary has been in use from the 12th cent. to the 2th cent. BC, following other authors from the 10th cent. on (Tsigarida 2008).

3 *Methods*

During field campaigns in September 2007 and 2008 32 boreholes were drilled along the coast of the Thermaikos Gulf using vibra-coring with an open window sampler (Table 1). Samples were retrieved after reaching maximum depths between 3 m and 8 m. The lithology, sedimentology and magnetic susceptibility of most cores from Angelochori, Epanomi and Sozopoli were already described by Reicherter et al. (2010) and therefore only a short summary will be provided supplemented by new data. Field work comprised detailed core description and additional holes were drilled to a total of 93 m.

A set of indicators are taken in account for the determination of tsunami deposits such as fining-and thinning-up sequences, rip-up clasts, mud-coated clasts, erosive bases, conservation status of biogenics, unusual faunal associations, the combination of sedimentological compounds with magnetic susceptibility und the inland distribution of the deposits (Dawson 1994, Dawson & Stewart 2007, Morton et al. 2007, Peters & Jaffe 2010, Reicherter et al. 2010, Bahlburg & Spiske 2011, Chagué-Goff et al. 2011, Courtney et al. 2012, Goff et al. 2012). Magnetic susceptibility was carried out with a Bartington MS2K-Sensor on open liner samples at 2 cm intervals. For wet sieving we used a Retsch AS 200 sieving machine. Residues of grain size analyses, fractions 0.063 mm –1 mm, were used for micropaleontological investigations from all cores. Samples from Mende were washed carefully over sieves with a minimum mesh size of 0.063 mm. Of 121 samples from all areas 54 contain foraminifera and the total number of foraminifera per sample is between 0 and 50 per 20 g sediment, except a single case (180).

Samples for radiocarbon dating (Table 3) were taken from Mende (area 6), Cape Epanomi north (area 2a) and Sozopoli (area 3, Fig. 1A). Radiocarbon dating was processed in 2008 at the Leibniz Labor für Altersbestimmung und Isotopenforschung, Christian-Albrecht-Universität Kiel. Radiocarbon dating from plant remains of B14-07 was conducted by BETA in 2018. Calibration was done with Oxcal software (Bronk Ramsey 2017) with the calibration database INTCAL 2013 (Reimer et al. 2013). Reservoir ages and ΔR values vary regionally and through time in the Aegean Sea and have a mean reservoir age for the Mediterranean of 390 ± 85 yrs (Facorellis & Vardala-Theodorou 2015). A reservoir age of 400 ± 40 years and ΔR 148 ± 40 for marine carbonate for shells from different sites of the Northern Aegean Sea (Pireaeus, Nafplion, Youra Island, Skyros Island) are taken into account (Reimer & McCormac 2002, Facorellis & Vardala-Theodorou 2015).

Directly north of the Poseidon sanctuary and behind the beach ridge (area 5) we drilled at 3 sites up to 4 m deep. The area belongs to a campsite inside a small forest (B13-08 in a flat depression (Fig. 2B), B14-08 and B 15-08 in clearings). Adjacent areas were not accessible due to private and military zones. The back slope at the beachward side of the sanctuary seems to be

Table 3. Results of radiocarbon dating and micropaleontological examination from the ancient Mende excavation (M1 – M8), cores B7-07 (Sozopoli) and B14-07 (Cap Epanomi). (Calibrating: oxcal software, Bronk Ramsey (2017), calibration curve IntCal13, Reimer et al. (2013), reservoir effect after Reimer & McCormac (2002), Facorellis & Vardala-Theodorou (2015)), bgl = below ground.

sample	**section**	**investigation**	**material**	**calibrated age in yrs BP (y AD), range: 2σ** δ13C	**micropaleontology**
M1	sect. 1a	microfossils	sand		shell debris
M2 KIA40178 HAM-3928	sect.1a	radiocarbon dating	charcoal	1032 – 1184 cal AD 919 – 767 cal BP δ13C: -24.55	
M2	sect.1a	microfossils	sand		shell debris of gastropods, relics of chitin, organic remains
M3	sect. 1a	radiocarbon dating	ceramics	–	
M4 KIA40175 HAM-3925	sect. 1b	radiocarbon dating	shell debris	811 – 626 cal BC (2760 – 2575 cal BP)	
M5 KIA40176 HAM-3926	sect 1a	radiocarbon dating	*Acanthocardium* sp.	736 – 521 cal BC (2685 – 2470 cal BP) δ13C: -2.51	
M6	sect. 1b	microfossils	fine sand		shell debris of various gastropods (fragments of cf.*Cylichna*), ostracods, agglutinated tubes
M7	sect. 1b	microfossils	sand		shell debris of gastropods and bivalves, organic remains, agglutinated tubes, aggl. foraminifers?
M8	sect. 2	microfossils	sand		shell debris of gastropods, plant remains, agglutinated tubes
Beta- 485871	B14-07 191-196 cm bgl	radiocarbon dating	woody material	776 – 971 cal AD (1174 – 979 cal BP) δ13C: –26.7 ‰	
Beta- 485870	B14-07 153-157 cm bgl	radiocarbon dating	woody material	602 – 674 cal AD (1348 - 1276 cal BP) δ13C: -27.0 ‰	
KIA40179 HAM-3929	B7-07 250 cm bgl	radiocarbon dating	soil	1545 – 1721 cal AD (405 – 229 cal BP) δ13C: -2.73	
KIA40180 HAM-3930	B7-07 385 cm bgl	radiocarbon dating	soil	3,849 – 3,602 cal BC (5,798 – 5,551 cal BP) δ13C: 14.81	

highly influenced by recent human activities and was not sampled. At the excavation (Mende, Fig. 2A) we took samples from three sections for micropaleontological investigations (Table 3). The upper 0.2 to 0.3 m of the sections consist of anthropogenic fill.

4 *Results from Kassandra peninsula*

4.1 *Ancient Mende*

At the Mende excavation (Fig. 2A, Fig. 3) the upper 0.2 m –0.3 m of section 1 consist of excavation debris underlain by soil with plant roots and fine, sandy slope debris. A marine layer occurs between terrestrial silty, fine sands at the base, between c. 1.87 m and 2.3 m bgl c. 1.10 m (section 1a) and 0.70 m (section 2) above sea level, respectively. Besides ceramics, fine sands contain charcoal and broken building materials, complete and partly articulated shells of bivalves like *Acanthocardium* sp. In sect.1 b (Fig. 3), the same layer splits into two fining-up sequences between 1.75 m and 2.45 m bgl, 1.25 m and 0.65 m above sea level, respectively. The lower sequence starts with gravels on top of an erosional base filling a shallow channel (Fig. 3), overlain by a second sequence with imbricated gravels at its base. A similar gravel deposit can be observed in sect. 2 on the opposite side of the excavation on top of silty sands and below excavation debris. Micropaleontological investigations of M1, M2 and M6 – M8 revealed small fragments of gastropods. Samples M6 and M7 also show fragments of agglutinated foraminifera and agglutinated worm tubes. In M6 fragments of small, thin-shelled gastropods of the marine species cf. *Cylichna* are found (Table 3). *Cylichna* lives as burrower in muddy seafloors on the lower shore or deeper. Sample M2 from the base of the overlying landslide in sect. 1a is dated to 1032–1184 cal AD (919–767 cal BP), the radiocarbon dating (M4, M5) near the base of the marine layer date to a time range from 811–521 cal BC (2760–2470 cal BP; Fig. 3, Fig. 6, Table 3).

4.2 *Possidi*

The uppermost 0.2 m – max. 0.5 m of the cores at Possidi consist of soil and moderately sorted, anthropogenically influenced, fine to medium sand. In B13-08 (fig. 4) clay and clayey silty sand with carbonate concretions occurs below soil at 0.25 m –0.95 m bgl. From 0.56 m to the total depth, the grain size increases generally from moderately to moderately well sorted sand, coarse sand and finally fine gravel that occurs from 2.50 m onwards. Sand and gravel show repeatedly fining-upward-sequences at 0.7 m –0.95 m, 2.33 m –2.51 m and a set of two graded sequences between 2.78 m to 3.24 m depth, which are all very poorly sorted at their base. Generally, a high content of plant remains and very small amounts of unidentified shell fragments occur.

B14-08 and B15-08 consist completely of middle to coarse sand and sandy gravels, with decreasing grain size to the top of the boreholes. Neither silt and clay nor distinct fining-up layers are observed and only some plant remains are common whereas shell debris is rare deeper than c. 0.8 m bgl.

Clays in B13-08 have carbonate concretions and from a depth of c. 2 m all boreholes sands are carbonatically cemented. The relatively high content of calcium carbonate is typical for recent beach sands from Possidi (Pyökäri & Lehtovaara 1993). As the cores are very similar, apart from the clayey interval, B13-08 is shown in Fig. 4 for all of them.

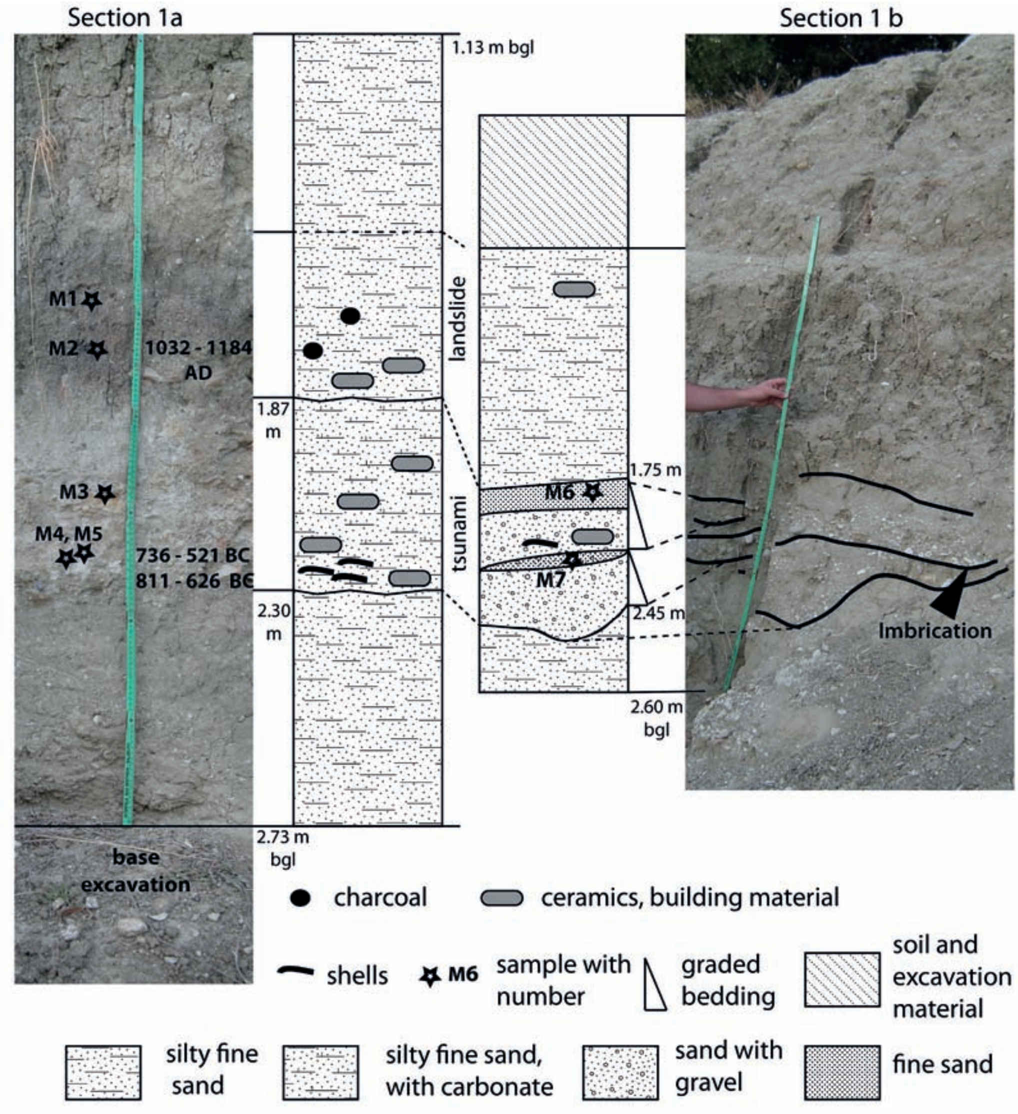

Fig. 3. Sample sites at the Ancient Mende excavation. For location of section 1 see Fig. 2A. The left side on the photo is dug 50 cm deeper into the slope than the right side. The channel structure continues into the slope.

Generally, magnetic susceptibility (Fig. 4) is relatively low (mean values 2–10) for all cores. Higher values occur in the clayey materials in B13-08 (≤ 56) only. Some small peaks occur but are caused by pebbles or occur at the top of the fining-up sequence in B13-08 (≤ 15 at 2.32 m). Carbonate cemented layers have zero magnetic susceptibility if clay and silt are absent. Quartz grains ≤ 0.5 mm are not rounded. All samples plot in the upper field of rolling transport in the CM diagram after Passega (1964) and Passega & Byramjee (1969).

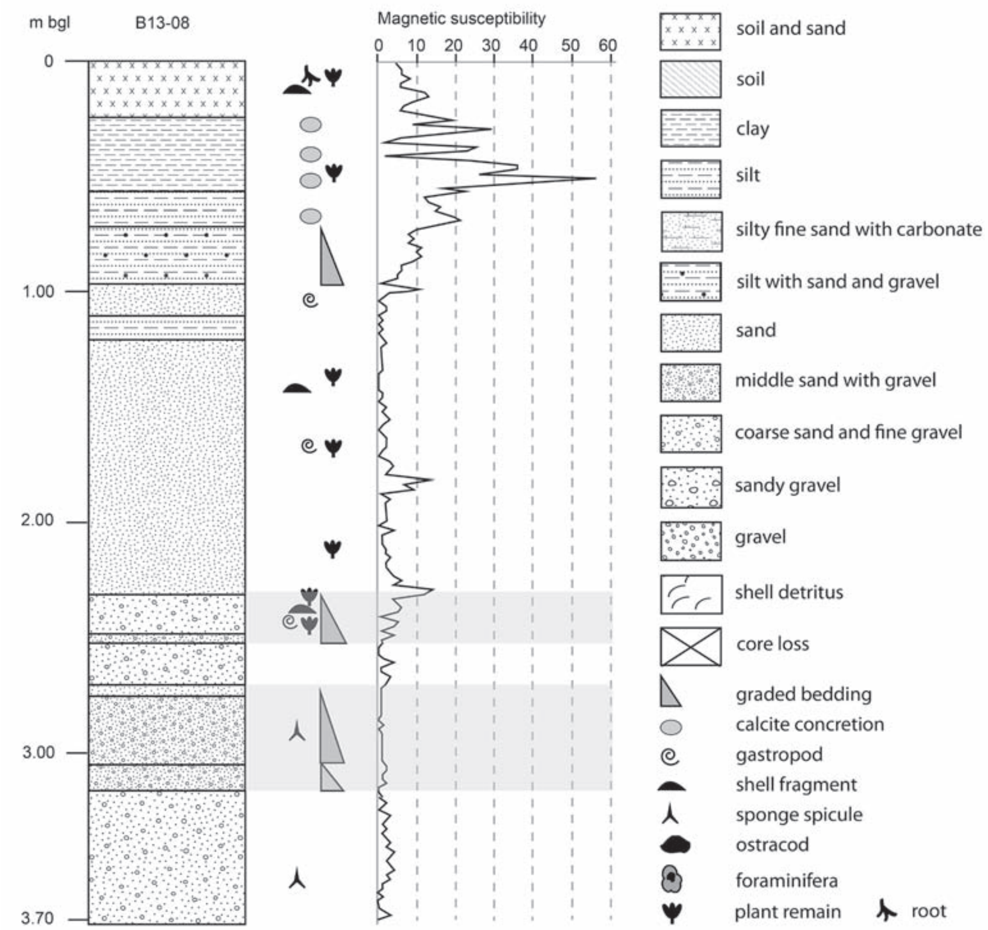

Fig. 4. Profile of core B13-08 from Possidi. Presumed event layers are highlighted in grey. bgl: below ground level. The legend also applies to Fig. 5.

Grain size analyses show no remarkable differences between sand and gravel of all cores. They are usually moderately sorted, but sorting increases within the fining up sequences. Transport mechanism indicating rolling transport applies to them all. Sediments are too coarse to guarantee adequate preservation of foraminifera and microfossils, therefore, the appearance of sponge spicules in two samples (B13-08 at 2.8 m – 2.88 m, fining-up sequence and 3.6 m – 3.72 m) is remarkable.

5 *Evidence of tsunami deposits between Angelochori and Potidea*

In the following, the results of earlier investigations from Reicherter et al. 2010 are briefly presented and supplemented by some more recent data which help to get a better idea of the distribution of EWE deposits along the coast of Chalkidiki.

5.1 *Angelochori*

Besides open marine beach sediments characterized by a heterogenic succession of alternating sands and gravels, well-preserved clayey lagoonal sediments are present in the upper half meter of B5-07 and B6-07 (Table 1). In B5-07, which is located 820 m from the beach, at 0.4 m –1.0 m and 1.10 m –1.8 m bgl two fining-up sequences of 0.6 m and 0.7 m thickness, with erosional bases, rip-up clasts of lagoonal mud and mud-coated clasts were found. Magnetic susceptibility is low in sands and gravel with considerable higher values in clayey (lagoonal) sediments and highest values in the fining-up sequences. In core B3-07, 400 m inland from the beach, a similar fining up layer with an erosive base occurs between 0.8 m –1.35 m bgl. These layers were interpreted as event deposits caused by paleotsunamis by Reicherter et al. (2010). While in B5-07 two event horizons have been preserved, in B3-07 it is only one, which can be explained by the proximity to the beach, where the conservation conditions are less favourable than in more distant areas.

The amount of foraminifera and their diversity in sediment cores from Angelochori is low (Table 4). The mean species in descending order are *Ammonia beccarii, Quinqueloculina seminula* and *Elphidium crispum* which prefer a coastal habitat (Table 4). The occurrence of *Ammonia tepida* together with *Elphidium crispum* in B3-07 between 1.25 m and 1.35 m can be interpreted as a clue to an event layer.

5.2 *Cape Epanomi*

Sediment cores from the upper beach (maximum distance to the shoreline 30 m) and the spit consist of alternating layers of poorly and very poorly sand and gravel of an open marine beach area, which are partly covered by windblown sands (Reicherter et al. 2010). Sediments are similar to those from Angelochori but with lower contents of gravels. In both areas (2a, 2b) in greater distance to the shoreline a lagoon developed with clayey and silty, occasionally sandy sediments with thicknesses between c. 1 m and 2 m. Foraminifers and microfossil are rare in all beach deposits, especially in the northern part (B13-07, B14-07), whereas their amount and diversity is notably higher in the southern part (B12-07, B16-07, Table 4). Samples from Epanomi, area 2b, reveal the highest amount and diversity of foraminifera (Table 4). *Ammonia beccarii, Elphidium crispum*, *Quinqueloculina* sp. and accompanying *Spiroloculina* sp. are the main species of the beach deposits. Clay and silt of the lagoonal facies are characterized by *Ammonia tepida*, *Haynesina* sp., *Aubignyna* sp. and well preserved ostracods.

The EWE deposit in core B14-07 (area 2a, Fig. 1A) is well preserved and recently dated by radiocarbon and therefore described in more detail (Fig. 5). Below soil and clay two fining-up sequences were drilled, which can be divided into 5 subunits. The lowest layer, (unit 1) has an erosional contact to poorly sorted, gravelly coarse sand of coastal origin with abundant plant remains and few shell fragments at 1.89 m. Unit 1 consists of a 0.06 m thick layer of very poorly sorted, disarticulated, sharp-edged bivalve shell detritus. Unit 2 is built of a fining-up sequence from gravel to sand above an erosive base. Unit 3 consists of a 0.02 m thick, fine gravel layer building the well-defined basal part of the upper fining-up sequence (unit 4) from coarse gravel to sand which is also rich in sharp-edged shell fragments and plant remains. At the top it changes with indistinct boundary into unit 5, consisting of c. 0.17 m rooted, carbonatic, clayey fine sand. Woody plant remains from below the base of the lower fining-up sequence (1.91 m

Table 4. Overview of contents of foraminfera, charophyts (indetermined) and ostracods (undetermined). Species and genera are listed separately in alphabetical order. 121 samples were taken, wherefrom 54 contain foraminifera. Interpretation of the environment is based on sample interpretation and the following literature:
1: Murray (1973), 2: Pujos-Lamy (1984), 3: Murray (1991), 4: Alve & Murray (2001), 5: Hohenegger & Baal (2003), 6: Barbero et al. (2004), 7: Fiorini (2004), 8: Morigi et al. (2005), 9: Murray (2006), 10: Frezza et al. (2010), 11: Holbourn et al. (2013).

Foraminifera/ microfossils	**Number of samples**	**Locality**				**facies**	**Tsunami deposit**
		Angelochori	**Cape Epanomi**	**Sozopoli**	**Nea Moudania**		
Ammonia beccarii	36	B3-07 (3) B4-07 (3) B5-07 (1) B6-07 (1)	B14-07 (1) B16-07 (4)	B7-07 (7) B9-07 (3) B20-07 (5) beach sand	B17-08 (7)	neritic - littoral	**Sozopoli** : B7-07, B9-07, B20-07
Ammonia tepida	22	B3-07 (2) B6-07 (1)	B12-07 (6) B16-07 (8) B14-07 (2)	B21-07 (1)	B17-08 (2)	lagoon	**Angelochori**: B3-07 **Cap Epanomi**: B14-07, B16-07 UE, B16-07 LE
Asterigerinata mammila	4	B4-7 (1)	B12-07 (3)			shallow marin (5,8,10)	
Asterigerina planorbis	3		B12-07 (2) B16-07 (1)			neritic - littoral	
Elphidium crispum	26	B3-07 (2) B4-07 (2)	B12-07 (4) B14-07 (1) B16-07 (2)	B7-07 (5) B9-07 (1) B20-07 (3) beach sand		neritic - littoral	**Angelochori**: B3-07, **Cap Epanomi**: B14-07 **Sozopoli**: B7-07, B9-07, B20-07
Elphidium fichtellianum	8	B4-07 (2)	B12-07 (2) B16-07 (2)	B20-07 (1) beach sand		littoral, estuarine (2)	
Elphidium granosum	6		B12-07 (3) B16-07 (3)			neritic, lagoons (9)	**Cap Epanomi**: B16-07 UE
Elphidium complanatum	3		B12-07 (2) B16-07 (1)			lagoonal environ-ment (6)	
Elphidium excavatum	1		B12-07 (1)			Littoral, > 100 m depth (9)	
Haynesina germanica	2		B12-07 (2)			lagoonal (9)	
Haynesina depressula	3		B12-07 (2) B16-07 (1)			lagoon, estuarine (9)	
Peneroplis pertusus	6	B4-07 (1) B5-07 (1) B6-07 (1)	B12-07 (2)	B7-07 (1) beach sand		shallow water, lagoon (9)	**Angelochori**: B5-07 UE
Quinqueloculina seminula	15	B3-07 (2) B4-07 (1) B6-07 (1)	B12-07 (3)	B7-07 (1) B9-07 (1) B20-07 (3) beach sand	B17-08 (3)	neritic - littoral	**Sozopoli**: B7-07, B9-07
Quinqueloculina bicarinata	5		B12-07 (2) B16-07 (2)		B17-08 (1)	neritic - littoral	

Quinqueloculina bradyana	1		B12-07 (1)			shallow marin [9]	
Quinqueloculina striata	3		B16-07 (2)		B17-08 (1)	littoral	
Quinqueloculina laevigata	1		B16-07 (1)			shallow marin [9]	
Quinqueloculina poeyana	1			B7-07 (1)		lagoon [9]	
Rosalina sp.	6	B4-07 (1)	B12-07 (5)			inner shelf, bathyal [1, 3,5]	
Rosalina bradyi	1	B3-7 (1)				shallow marin [9]	
Siphonaperta aspera	1			B7-07 (1)		infralitto-ral [7]	
Trochammina inflata	2		B12-07 (2) B16-07 (2)			neritic - brackish [9, 11]	
Triloculina trigonula	3			B20-07 (1) beach sand	B17-08 (1)	lower neritic [5]	**Sozopoli**: B20-07
species	22	8	18	9	7		7
Adelosina sp.	4		B12-07 (2) B16-07 (2)			infralitto-ral [7]	**Cap Epanomi**: B16-07 UE
Aubignyna sp.	7		B12-07 (2) B16-07 (4) B14-07 (1)			shallow water, lagoons [4,9]	**Cap Epanomi**: B16-07 UE
Haynesina sp.	9		B12-07 (1) B16-07 (4) B14-07 (1)	B9-07 (1) B21-07 (1)	B17-08 (1)	finegrained sediments, euryhalin [9]	**Cap Epanomi**: B16-07 UE **Sozopoli**: B9-07
Massilina sp.	7		B12-07 (3)	B7-07 (1)	B17-08 (3)	inner shelf , photic zone [9]	
Quinqueloculina sp.	4		B12-07 (1) B16-07 (1)	B20-07 (1) beach sand		inner shelf - lagoon [1,3,5]	
Spiroloculina sp.	8		B12-07 (1) B16-07 (6)	beach sand	B17-08 (1)	shallow marin - lagoon [9]	**Cap Epanomi**: B16-07 UE
Ostracoda	35	B3-07 (3) B4-07 (1) B5-07 (1)	B12-07 (3) B14-07 (1) B16-07 (6)	B7-07 (7) B9-07 (3) B20-07 (4) B21-07 (6)		lagoon	**Cap Epanomi**: B14-07 B16-07 UE, B9-07, B20-07
Charophyta	15	B3-07 (1) B4-07 (1) B5-07 (1) B6-07 (1)	B12-07 (1) B15-07 (1)	B7-07 (2) B9-07 (3) B21-07 (4)		lagoon	**Sozopoli**: B7-07

–1.96 m) give an age of 776–971 yrs cal AD (1174–979 yrs cal BP). The age dated from woody remains from the central part of the upper fining-up sequence (unit 3) is 602–674 yrs cal AD (1348–1276 yrs cal BP) (Table 3, Fig. 6).

Magnetic susceptibility values of the tsunami deposits range between 0 and 10 with a single peak (235) at the base of the shell layer (unit 1), while the overlaying clay has values between 15

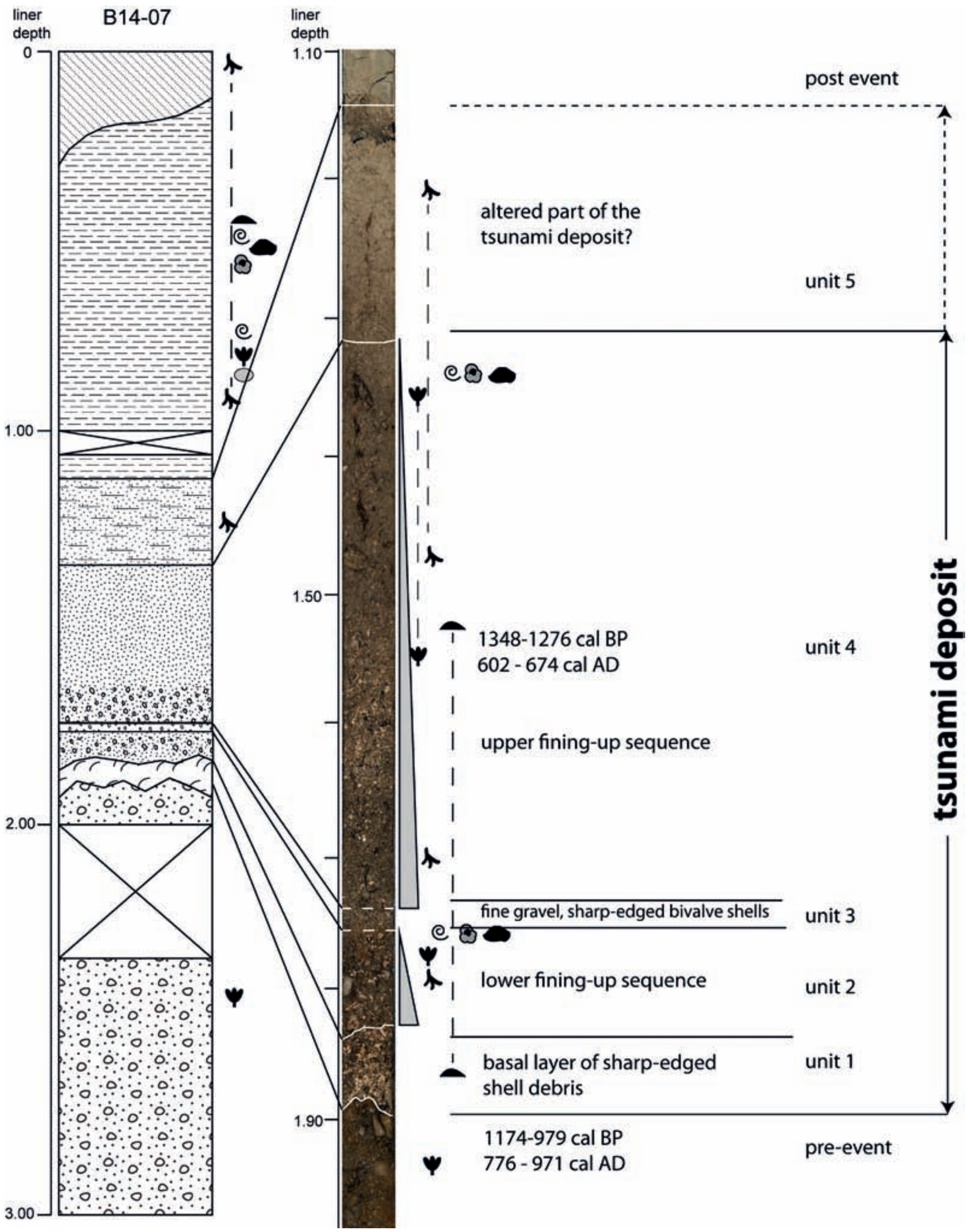

Fig. 5. Profile of core B14-07 with a scaled up photo of the tsunami horizon. For legend see Fig. 4.

and 30. A sample taken near the base of the upper sequence contains broken ostracods, gastropods (*Cerithium* and Hydrobiidae), *Elphidium crispum, Ammonia tepida*, many plant remains and abundant shell fragments. Between 1.36 m –1.45 m bgl Hydrobiidae, broken ostracods, juvenile bivalves and *Ammonia tepida*, and between 1.67 m –1.74 m *Ammonia beccarii*, *Ammonia tepida*, roots, plant remains and broken ostracods occur. Nearly all microfossils show traces of strong abrasion. The co-occurrence of organisms from coastal and lagoon areas (Table 4) is interpreted to be caused by an event. Donato et al. (2008) interpret the accumulation of strong angular fragmentation like in unit 1 as a result of turbulent flow during a tsunami. Similar layers are also described by Bahlburg & Spiske (2011) as tsunamigenic inflow deposits. Due to the fine sand, Ca content missing in the clay above, lower magnetic susceptibility and the root penetration, we assume that unit 5 was deposited by a tsunami and later altered by vegetation as observed in modern tsunamis (Szczucinski 2012). The tsunami layer can be correlated with a fining-up sequence in B13-07 (1.58 m –1.98 m depth), containing intraclasts and small pieces of charcoal.

From the southern part (B16-07) two fining-up sequences with erosive bases containing rip up clasts, mud-coated clasts and articulated *Acanthocardium* sp. occur between 2.38 m and 3.7 m bgl which characterize them as paleotsunami deposits. This fining-up sequences are clearly separated by 0.38 m of sand and a carbonate crust (Reicherter et al. 2010).

5.3 *Sozopoli*

The sediment cores near Sozopoli (area 3, Fig. 1A) have the thickest accumulation of lagoonal clays and silts with increasing layer thickness from west to east. Gypsum and dark laminated mud represent the deeper lagoonal deposition in B7-07 (> 5 m depth bgl) and B9-07 (below 3.5 m bgl, Reicherter et al. 2010). Into these lagoonal deposits beach sand and gravel are intercalated with thickness decreasing from west to east (Reicherter et al. 2010). The foraminiferal distribution of the beach sediments is similar to the Angelochori area with *Ammonia beccarii*, *Elphidium crispum* and *Quinqueloculina seminula*, (Table 4) whereas in lagoonal sediments mainly ostracods, charophyta and few *Ammona tepida* were found. An event layer was identified in a coastal parallel profile through three cores (B7-07, B9-07, B20-07, Table 3) by Reicherter et al. (2010) evidenced by erosive bases, mud-coated clasts, rip-up clasts and fining- and thinning-up sequences and in B7-07 by so-called tsunami wave train deposits. The first erosional base occurs at a depth of 3.65 m (B7-07), 2.85 m (B9-07) and, 3.15 m (B20-07). The thickness of the event layer decreases from 1.23 m to 0.61 m from west to east. The indication by foraminifera of a tsumani is low, but the presence of charophytes together with foraminifera from the littoral milieu in the sands of the event layer (B7-07, Table 4) can be taken as evidence of an EWE-event. Two samples from B7-07 were dated by radiocarbon (Table 3). The beach sand below the tsunami deposit has an age between 3849 and 3602 cal BC (5798–5551 cal BP). Material from the upper (third) graded sequence is much younger and is dated to an age between 1545–1721 cal AD (405–229 cal BP). However, this sample seems to be contaminated, and the age will be discarded (see discussion).

5.4 *Nea Moudania*

South of Nea Moudania (area 4, Fig. 1A) the sediments resemble Angelochori and Cape Epanomi observations with mainly fine to coarse, moderately to poorly sorted beach sands and gravel but clayey silts and clays occur only as rare intercalations of max. 20 cm thickness. In B21-08 beach sediments are replaced by very poorly sorted, reddish gravel and coarse sands below c. 4.20 m, wherein shell debris is missing. Foraminifera and microfossils are very rare and occur in B17-08 only, minor indeterminable debris in B23-08. Main species of the littoral zone are *Ammonia beccarii* and *Quinqueloculina seminula* as in areas 1 to 3 too. Several fining-up sequences with erosive bases within sandy beach deposits occur in B17-08, B21-08 and B23-08 but particular characteristics for a tsunami-related origin like mud-coated clasts, rip-up clasts, mixing of microfossils from different environments as found in Angelochori, Epanomi and Sozopoli are missing. Of special interest are graded intercalations of fine gravels, sands and silts with erosional contact to the base and the top in B23-08 between 1.59 m –1.68 m and 1.89 m –1.99 m bgl within lagoonal sediments. Magnetic susceptibility and Ca content are significantly higher and Fe content is significantly lower than in the clay above and beneath. In B21-08 a fining-up sequence with erosional base and a thin clay layer at its top is observed between 2.32 m and 2.49 m bgl. These horizons are tentatively interpreted as a high-energy layer.

6 *Interpretation and discussion*

The marine layer at the Mende excavation shows an event layer characterized by fining-up sequences, erosive contacts and the occurrence of a channel-like bed with an imbricated gravel layer (Fig. 3), which occurs inside the building area. The small, asymmetrical channel-like form grades laterally into the marine layer. Its base scours c. 10 cm deep into the underlying sediment and is filled with two fining-up cycles with shell debris from marine bivalves and gastropods and fine sand. The imbrication of gravel indicates a short phase of strong water currents. Similar erosional features were described by Bahlburg & Spiske (2011) from a recent tsunami in Chile. Therefore this channel is interpreted as a backwash channel, which was formed early, perhaps after the first wave and then filled by the following waves. The interpretation of the marine layer as tsunami deposit is also confirmed by the occurrence of small maritime gastropods from silty and muddy environments as can be found southward from the spit in deeper parts of the shelf. Ages from the base of the marine sequence are older than the 479 BC tsunami described by Herodotus as the material originate from the settlement after 800 years BC and before around 500 years BC (Fig. 6). It can be assumed that the dated material is from the erosion caused by the tsunami (*terminus ante quem*, as all is older than the layer). The post event sediments are much younger with around 1100 yrs AD. Taken in account the sedimentary structures, marine endobenthic snails and the age of the reworked material, this event horizon may originate from the "Herodotus" tsunami.

At Possidi there are no layers that resemble those of EWE described from Angelochori, Cap Epanomi and Sozopoli by Reicherter et al. (2010) but sediment core B13-08 (Fig. 4) yields evidence. It shows an overall fining-up from gravel to clay which reflects the transition from a beach environment at the foot of the small hill to a small lagoonal area behind the spit of Possidi.

Table 5. Occurrence of verified and supposed tsunami deposits along the eastern coast of the Thermaikos Gulf (Chalkidiki). Data from (1) Reicherter et al. (2010), (2) Smid (1970) and this paper. For number of locations see Fig. 1A, bgl: below ground level.

Location	Outcrop ID	Distance to the recent coast	Situation	Depth Event layer bgl (m)	Events
(1) Angelochori, drilling	B5-07(1)	700 m	lagoonal area	0.40 – 1.00 1.10 – 1.80	upper event lower event
	B3-07(1)	c. 400 m		0.80 – 1.35	event
(2) Cap Epanomi, drilling	B16-07(1)	800 – 1000 m	lagoonal area	2.38 – 2.62 3.00 – 3.70	upper event lower event
	B13-07	c. 300 m		1.58 – 1.98	event
	B14-07	360 m		1.32 – 1.89	event
(3) Sozopoli village, drilling	B7-07(1), B9-07(1), B20-07(1)	145 m 170 m 100 m	former? lagoonal area	2.42 – 3.65 c. 1.60 – 2.85 2.54 – 3.15	event
(4) Nea Moudania, drilling	B21-08	200 m	flat area behind the beach	2.32 – 2.49	event layer?
	B23-08	100 m		1.59 – 1.68 1.89 – 1.99	upper event lower event
(5) Possidi, drilling	B13-08	200 m	flat area behind the beach	2.33 – 2.51 2.78 – 3.24	events of unproven origin
(6) Mende	excavation	100 m	antique greek settlement	1.79 – 2.45	479 BC *"Herodotus tsunami"*
Ancient Potidea	historical tradition(2)	phenomena observed at the coast	coastal area		479 BC *"Herodotus tsunami"*

Characteristics typical of tsunami deposits seem to be absent such as erosive bases, mud caps, or unusual faunal associations. Rip-up clasts do not occur because there are no fine-grained, i.e. lagoon deposits, nearby. The erosional impact of tsunamis in littoral areas is high and much material can be eroded directly from the coastal zone (Dawson 1994). For Possidi this makes it difficult to distinguish coastal sediments from tsunami deposits of the same origin without additional parameters. Furthermore, the exposure of the Possidi spit towards the currents entering the Thermaikos Gulf from the Aegean Sea and the exposure to the Etesians from the North seem to reduce the potential for the preservation of tsunami deposits. The lower sequences between 2.33 m to 2.51 m and 2.78 m to 3.24 m are candidates for EWE.

The fining-up sequences alone, which in every interval get better sorted to the top, are not characteristic to be identified as tsunami. But on one side there is a higher magnetic susceptibility at the top of the fining-up sequence at 2.33 m, on the other side this sequence contains a mixing of terrestrial plant remains and marine shell fragments. Both observations may point at a backwash deposit. Repeating fining-upward like observed between 2.78 m to 3.24 m is also unusual for storm depositions and is more often interpreted as a tsunamigenic feature (Tuttle et al. 2004, Morton et al. 2007, Chagué-Goff et al. 2011). In outer-Mediterranean regions, tropical storms and tsunamis may generate identical features (Engel & Brückner 2011) but in the Mediterranean, storms with Beaufort 12 are not expectable nor have been observed and

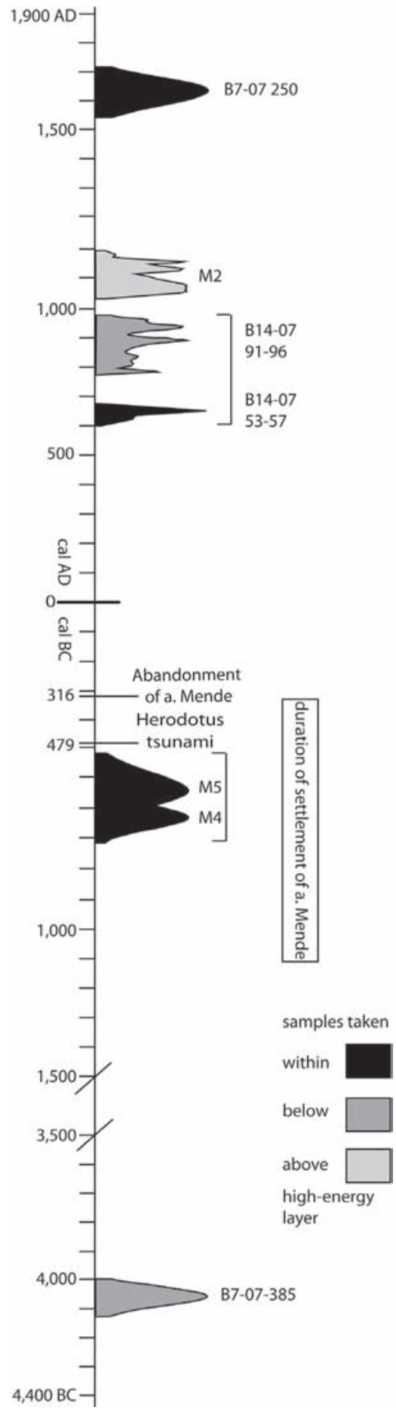

Fig. 6. Time line of ages of high energy layer and concomitant sediments. Peaks of calibrated ages are not to scale. The 2σ probability range is given. For sample information see Table 3.

tsunamis turned out to be much more costly and deadlier than storms (see discussion by Vött et al. 2018). As a conclusion the sediments are deposited during a EWE and may be rather deposited by a tsunami than a storm.

Most layers we interpreted as tsunami are preserved in areas with a distance from minimum c. 100 m to c. 1000 m (Table 5) from the recent shoreline, to far inland to be storm deposits (Morton et al. 2007, Chague-Goff et al. 2011), where sites are sheltered from wave action, currents and fluvial erosion. Except of the areas around Sozopoli and Nea Moudania two events are found which show evidence of tsunami deposits (Table 5). Regarding the core depth of the paleotsunami deposits, measured from the top of the event layer, tsunami evidence is recurrent below 1 m depth bgl with the exception of Angelochori (B5-07) where high-energy deposits occur between 0.4 m –1 m depth. The erosive bases of the other event layers occur at three mean depths, c. 1.80 m, c. 2.60 m and c. 3.40 m, with no obvious relation to the locality. The cause for the different depths can be the age of the event, the original morphology and the strength of the erosion associated with the event. Positive vertical displacement is described by Pavlopoulos et al. (2011) for Thessaloniki and Epanomi, which can also influence the burial depth of the layers. If two event deposits were drilled, 0.1 m to 0.38 m of background sediment separates the layers. Table 5 lists the distribution of possible tsunami layers along the eastern coast of the Thermaikos Gulf and gives a compilation of our data.

The calibrated ages from B14-07 (Cape Epanomi, area 2a, Fig. 6) and B7-07 (Sozopoli, area 3, Fig. 6), where in each case only one event was found, are strongly different. Ages from woody material of the high-energy event layer of B14-07 range from 776–971 cal AD (1174–979 yrs BP) and are therefore older than the woody material from directly below the base of the sequence. This may indicate contamination or possibly the effect of strong erosion associated with the event reworking older plant and wood remains. Ages from B7-07 show that sands below the high-energy event are older than 5,500 years whereas the upper interval (third fining-up sequence) is dated to 405–229 cal yrs BP (1545–1721 cal AD) so this would be a very young event. The 2 m thick lagoonal clay cover formed at the earliest after 405 cal yrs BP to 229 cal yrs BP, resulting in a sedimentation rate of 0.4 cm/yr to 0.8 cm/yr. Therefore the age is not regarded as reliable and was discarded.

The 479 BC tsunami is historically recorded and was assumedly caused by a possible submarine slump or a meteorological effect after Ambraseys (2009), however, also an earthquake can be the causative event (Reicherter et al. 2010). At Mende the effects of the tsunami could be verified but which of the other observed event layers belongs also to this tsunami, is unclear and the younger event observed near Epanomi is not mentioned in the historical tsunami catalogues between 479 BC and 1983 for the investigation area (Table 1).

7 *Summary and conclusions*

Along the eastern coast of the Thermaikos Gulf sediment cores from areas 1–3 show a similar development from lagoonal areas to a beach environment, which become lagoonal area again when they are closed off from the sea. Dried out lagoons are covered with aeolian sand, soil or anthropogenic infill (Reicherter et al. 2010). In area 4 (Nea Moudania, Fig. 1A) no early lagoonal sedimentation is observed and as the coastal relief rises to the south, the thickness of lagoon like sediments decreases from 1.65 m at B23-08 (area 4) to zero at Possidi (area 5), reducing the preservation potential of high energy deposits. Tsunami deposits published by Reicherter et al. (2010) were affirmed, dated and traces of tsunami deposits now are found at the whole coast of the Thermaikos Gulf from Angelochori to Kassandra peninsula. Evidence for minimum two different event layers on the coasts of Chalkidiki was found at several sites from north to south (Table 5). One of them, at Mende, was related to the 479 BC tsunami described by Herodotus. A younger one, near Cape Epanomi, dates back to the time between 602 cal AD to 971 cal AD (Fig. 6). The relevant databases do not have information about those tsunamis or related deposits (Table 1).

The preservation of tsunami deposits highly depends on areas sheltered from erosion by wave, wind action and currents like in lagoonal areas, estuaries, area without strong fluvial influence and areas out of reach of storm and flooding events. Post tsunami vegetation can also destroy deposits as it is presumed for the upper part of the event layer in B14-07 (unit 5, Cap Epanomi, Fig. 5). In areas where event deposits are exposed to human activities, geological information is blurred or got lost completely. But careful correlation of unsure event horizons with such of sure tsunami layers may allow mapping the extent of paleotsunamis. The investigation area of Possidi north of the Poseidon sanctuary has a constrictive potential for preserving tsunami deposits whereas a lagoonal area, like especially at B20-07, has best conditions. However, how the example from Mende shows, settlements have their own potential to conserve backwash sediments as well as draining and flooding features caused by a tsunami.

We presented traces of the *"Herodotus tsunami"* and it should be feasible to look for traces of natural hazards at different ancient sites in order to correlate event layers. More insights in the history of the sanctuary and some more investigation on other parts of the coast of Kassandra peninsula could help to complete our knowledge on coastal hazards in this region. Our investigations testify to the "little seed of truth" in mythical and ancient histories and sagas, not only along the Northern Aegean coast, in order to complete the history of paleotsunamis in the Thermaikos Gulf area.

Acknowledgements

We are thankful for the help of our drilling team Simon Virgo, Marc Fröwis, Fabian Syberberg and Christoph Grützner and financial support provided by the IKYDA project of the DAAD.

References

Ainian, A. M. & Leventi, I. (2009): The Aegean. – In Raaflaub, K. A. & van Wees, H. (eds): A companion to Archaic Greece. – Blackwell, 212–238.

Altinok,Y., Alpar, B., Özer, N. & Aykurt, H. (2011): Revision of the tsunami catalogue affecting Turkish coasts and surrounding regions. – Nat. Hazards Earth Syst. Sci. **11** (2): 273–291.

Alve, E. & Murray, J. W. (2001): Temporal variability in vertical distributions of live (stained) intertidal forainifera, Southern England

. – J. Foraminiferal Res. **31** (1): 12–24.

Ambraseys, N. (2009): Earthquakes in the Mediterranean and Middle East. – A multidisciplinary Study of Seismicity up to 1900. – Cambridge University Press, Cambridge, 947 pp.

Bahlburg, H. & Spiske, M. (2011): Sedimentology of tsunami inflow and backflow deposits: key differences revealed in a modern example. – Sedimentology, https://doi.org/10.1111/j.1365-3091.2011.01295×.

Barbero, R. S., Albani, A. D. & Bonardi, M. (2004): Ancient and modern salt marshes in the Lagoon of Venice. – Palaeogeogr. Palaeoclimatol. Palaeoecol. **202:** 229–244.

Bolt, B. A. (1978): Earthquakes. – W. H. Friedman & Company, New York, 241 pp.

Bourgeois, J. & Weiss, R. (2009): "Chevrons" are not mega-tsunami deposits – A sedimentologic assessment. – Geology **37** (5): 403–406.

Bronk Ramsey, C. (2017): Methods for Summarizing Radiocarbon Datasets. – Radiocarbon **59 (**2): 1809–1833.

Chagué-Goff, C., Schneider, J.-L., Goff, J. R., Dominey-Howes, D. & Strotz, L. (2011): Expanding the proxy toolkit to help identify past events. – Lessons from the 2004 Indian Ocean Tsunami and the South Pacific Tsunami. – Earth-Sci. Rev., doi: 10.1016/j.earscirev.2011.03.007.

Courtney, C., Dominey-Howes, D., Goff, J., Chagué-Goff, C., Switzer, A. D. & McFadgen, B. (2012): A synthesis and review of the geological evidence for palaeotsunamis along the coast of southeast Australia: The evidence, issues and potential ways forward. – Quat. Sci. Rev. **54:** 99–125.

Dawson, A. G. (1994): Geomorphological effects of tsunami run-up and backwash. – Geomorphology **10:** 83–94.

Dawson, A. G. & Stewart, I. (2007): Tsunami deposits in the geological record. – Sediment. Geol. **200:** 166–183.

Donato, S. V., Reinhardt, E. G., Boyce, J. I., Rothaus, R. & Vosmer, T. (2008): Identifying tsunami deposits using bivalve shell taphonomy. – Geology **36** (3): 199–202.

Engel, M. & Brückner, H. (2011): The identification of paleo-tsunami deposits – a major challenge in coastal sedimentary research. – In: Karius, V., Hadler, H., Deicke, M.,von Eynatten, H., Brücker, H. & Vött, A. (eds): Dynamische Küsten – Prozesse, Zusammenhänge und Auswirkungen. – Coastline Reports **17:** 65–80.

Facorellis, Y. & Vardala-Theodorou, E. (2015): Sea surface radiocarbon reservoir age changes in the Aegean Sea from about 11,200 BP to present. – Radiocarbon **57** (3): 493–505, doi: 10.2458/azu_rc.57.18363.

Fiorini, F. (2004): Benthic foraminiferal associations from Upper Quaternary deposits of southeastern Po Plain, Italy. – Micropaleontology **50 (**1): 45–58.

Frezza, V., Pignatti, J. S. & Matteucci, R. (2010): Benthic foraminiferal biofacies in temperate carbonate sediment in the Western Pontine Archipelago (Tyrrhenian Sea, Italy). – J. Foraminiferal Res. **40** (4): 313–326.

Goff, J., Chagué-Goff, Ch., Nichol, S., Jaffe, B. & Dominey-Howes, D. (2012): Progress in palaeotsunami research. – Sediment. Geol. **243–244:** 70–88.

Guy, M., Bornovas, J., Bizon, G. & Zaronikas, I. N. (1969): 1:50.000 Geological map of Greece, "Sheet Peninsula of Kassandras". – Institute for Geology and Subsurface Research.

Hohenegger, J. & Baal, C. (2003): 3. Protisten (Mikroalgen und Protozoen) – Klasse Foraminiferea d'Orbigny, 1826. – In: Hofrichter, R. (ed.): Das Mittelmeer – Fauna, Flora, Ökologie – Band **II**/1: Bestimmungsführer – Prokaryota, Protista, Fungi, Algae, Plantae, Animalia (bis Nemertea): 124–135, Spektrum Akademischer Verlag.

Herodotus (unknown year): The Historie Book 8: Urania, chapter 129. – English translation Godley, A. D. (1920).

Hofrichter, R., Kern, W., Beckel, L., Domnig, I., Zankl, A. & Hein, A. (2002): Geographie und Klima. – In: Hofrichter, R. (ed.): Das Mittelmeer **I:** 102–195, Spektrum Akademischer Verlag.

Holbourn, A., Henderson, A. S. & MacLeod, N. (2013): Atlas of Benthic Foraminifera. First edition. – Wiley, 642 pp.

Lalechos, N. & Bizon, G. (1969): 1:50.000 Geological map of Greece, "Sheet Epanomi" – Institue of Geological and Mining Research.

Maramai, A., Brizuela, B. & Graziani L. (2014): The Euro-Mediterranean Tsunami Catalogue. – Ann. Geophys. Italy **57** (4): 26 pp, doi:10.4401/ag-6437.

Mollat, H., Antoniades, P., Ricou, L. E., Christodoulou, G., Parginos, D., Kourmoulis, N., Gillet, S., Marinos, G., Yannoulis, P. & Sotiriades, L. (1978): 1:50.000 Geological map of Greece, "Sheet Vasilika". – Institute of Geological and Mining Research.

Morigi, C., Jorissen, F. J., Fraticelli, S., Horton, B. P., Principi, M., Sabbatini, A., Capotondi, L., Curzi, P. V. & Negri, A. (2005): Benthic foraminiferal evidence for the formation of the Holocene mud-belt and bathymetrical evolution in the central Adriatic Sea. – Marine Micropaleontology **57:** 25–49, doi:10.1016/j.marmicro.2005.06.001.

Morton, R. A., Gelfenbaum, G., Jaffe, B. E. (2007): Physical criteria for distinguishing sandy tsunami and storm deposits using modern examples. – Sediment Geol. **200:** 184–207.

Moschonissioti, S. (1998): Excavation at Ancient Mende. – In: Bérard, J. (ed.): Euboica: L'Eubea e la presenza euboica in Calcidica e in Occidente [en ligne]. – Naples: Publications du Centre (généré le 04 janvier 2016), http://books.openedition.org/pcjb/661.

Murray, J. W. (1973): Distribution and Ecology of Living Benthic Foraminiferids. First edition. – Heinemann Educational Books, London, 274 pp.

Murray, J. W. (1991): Ecology and Palaeoecology of Benthic Foraminifera. First edition. – Longman Scientific & Technical, United Kingdom, New York, 402 pp.

Murray, J. (2006): Ecology and Applications of Benthic Foraminifera. First edition. – Cambridge University Press, Cambridge, 426 pp.

National Geophysical Data Center / World Data Service: NCEI/WDS Global Historical Tsunami Database. NOAA National Centers for Environmental Information, doi:10.7289/V5PN93H7 [3.1.2019].

Necmioglu, O. & Özel, N. M. (2015): Earthquake Scenario-Based Tsunami Wave Heights in the Eastern Mediterranean and Connected Seas. – Pure Appl. Geophys., doi 10.1007/s00024-015-1069-y.

Papadopoulos, G. A. (2002): Tsunamis in the East Mediterranean: A Catalogue for the Area of Greece and Adjacent Seas. – Proceedings of the International Workshop on Tsunami Risk Assessment beyond 2000: Theory, Practice and Plans. – Moscow, Russia, 34–42.

Papadopoulos, G. & Chalkis, B. J. (1984): Tsunamis observed in Greece and the surrounding area from antiquity up to present times. – Mar. Geol. **56:** 309–317.

Papadopoulos, G. A. & Fokaefs, A. (2005): Strong tsunamis in the Mediterranean Sea: a re-evaluation. – ISET Journal of Earthquake Technology **42:** 159–170.

Papadopoulos, G. A., Gràcia, E., Urgeles, R.,Sallares, V., De Martini, P. M., Pantosti, D., González, M., Yalciner, A. C., Mascle, J., Sakellariou, D., Salamon, A. & Tinti, St., Karastathis, V., Fokaefs, A., Camerlenghi, A., Novikova, T. & Papageorgiou, A. (2014): Historical and pre-historical tsunamis in the Mediterranean and its connected seas: Geological signatures, generation mechanisms and coastal impacts. – Mar. Geol., doi: 10.1016/j.margeo.2014.04.014.

Papanikolaou, I. D. & Papanikolaou, D. I. (2007): Seismic hazard scenarios from the longest geological constrained active fault of the Aegean. – Quat. Int. **171–172:** 31–44.

Papazachos, B. C. & Papazachou, C. (1997): The earthquakes of Greece. – Ziti Publ., Thessaloniki, Greece, 304 pp.

Passega, R. (1964): Grain size representation by CM patterns as a geological tool. – J. Sed. Pet. **34** (4): 830–847.

Passega, R. & Byramjee, R. (1969): Grain size image of clastic deposits. – Sedimentology **13:** 233–252.

Pavlopoulos, K., Kapsimalis, V., Theodorakopoulou, K. & Panagiotopoulos, I. P. (2011): Vertical displacement trends in the Aegean coastal zone (NE Mediterranean) during the Holocene assessed by geo-archaeological data. – The Holocene **22** (6): 12 pp., doi: 10.1177/0959683611423683.

Peters, R. & Jaffe, B. E. (2010): Identification of tsunami deposits in the geologic record; developing criteria using recent tsunami deposits. – U.S. Geol. Survey, Open-file report 2010–1239: 39 pp, https://pubs.usgs.gov/of/2010/1239/of2010-1239.pdf.

Poulos, S. E., Chronis, G. Th., Collins, M. B. & Lykousis, V. (2000): Thermaikos Gulf Coastal System, NW Aegean Sea: an overview of water/sediment fluxes in relation to air-land-ocean interactions and human activities. – J. Mar. Syst. **25:** 47–76.

Pujos-Lamy, A. (1984): Foraminiferes benthiques et bathymetrie: Le Cenozoique du Golfe de Gascogne. – Palaeogeogr. Palaeoclimatol. Palaeoecol. **48:** 39–60.

Pyökäri, M. & Lehtovaara, J. J. (1993): Beach material and its transport in accordance with the predominant and prevailing wave directions on some shores in northern Greece. – J. Coastal Res. **9** (3): 609–627.

Reicherter, K., Papanikolaou, I., Roger, J., Mathes-Schmidt, M., Papanikolaou, D., Rössler, S., Grützner, C. & Stamatis, G. (2010): Holocene tsunamigenic sediments and tsunami modelling in the Thermaikos Gulf area (northern Greece). – Z. Geomorphol. **54**, Suppl. 3: 99–126.

Reimer, P. J. & McCormac, F. G. (2002): Marine radiocarbon reservoir corrections for the Mediterranean and Aegean Seas. – Radiocarbon **44** (1): 159–166.

Reimer, P. J., Bard, E., Bayliss, A., Beck, J. W., Blackwell, P. G., Bronk Ramsey, C., Grootes, P. M., Guilderson, T. P., Haflidason, H., Hajdas, I., Hattz, C., Heaton, T. J., Hoffmann, D. L., Hogg, A. G., Hughen, K. A., Kaiser, K. F., Kromer, B., Manning, S. W., Niu, M., Reimer, R. W., Richards, D. A., Scott, E. M., Southon, J. R., Staff, R. A., Turney, C. S. M. & van der Plicht, J. (2013): IntCal13 and Marine13 Radiocarbon Age Calibration Curves 0–50,000 Years cal BP. – Radiocarbon, **55** (4): 1869–1887.

Smid, T. (1970): Tsunamis in Greek Literature. – Greece and Rome **17** (1): 100–104, doi:10.1017/S0017383500017393.

Stillwell, R., MacDonald, W. L. & McAlister, M. H. (ed.) (without year): POTEIDAIA (Nea Poteidaia) Chalkidike, Greece. – The Princeton Encyclopedia of Classical Sites, http://www.perseus.tufts.edu/hopper/text?doc = Perseus:text:1999.04.0006:entry=poteidaia) [accessed 06-14-2017].

Soloviev, S. L. (1990): Tsunamigenic Zones in the Mediterranean Sea. – Nat. Hazards **3:** 183–202.

Soloviev S. L., Solovieva O. N., Go, C. N., Kim, K. S. & Shchetnikov, N. A. (2000): Tsunamis in the Mediterranean Sea 2000 B. C. – 2000 A. D. – Springer, Advances in Natural and Technological Hazards Research **13:** 237 pp.

Szczuciniski, W. (2012): The post-depositional changes of the onshore 2004 tsunami deposits on the Andaman Sea coast of Thailand. – Nat Hazards **60:** 115–133.

Tiverios, M. (2008): Greek Colonisation of Northern Aegean. – In Tsetskhladze, G. R. (ed.): Greek colonisation. An account of Greek colonies and other settlements overseas **2:** 1–154, Cambridge University Press, Cambridge.

Tsigarida, B. (2008): Chalcidice. – In: Lane Fox, R. J. (ed.): Brill's Companion to Ancient Macedonia. Studies in the Archaeology and History of Macedon, 650 BC –300 AD: 137–158; Brill Academic Pub, Leiden/Boston.

Tuttle, M. P., Ruffman, A., Anderson, Th. & Jeter, H. (2004): Distinguishing Tsunami from Storm Deposits in Eastern North America. – The 1929 Grand Banks Tsunami versus the 1991 Halloween Storm. – Seismol. Res. Lett. **75** (1): 117–131.

U.S. Geological Survey (USGS) (2014): Shuttle Radar Topography Mission, 1 Arc-Second scenes N39E022V3, N39E023V3, N39E024V3,N40E022V3, N40E023V3, N40E024V3. Earth Resources Observation and Science (EROS) Center.

Vött, A., Bruins, H. J., Gawehn, M., Goodman-Tchernov, B. N., De Martini, P. M., Kelletat, D., Mastronuzzi, G., Reicherter, K., Röbke, B. R., Scheffers, A., Willershäuser, T., Avramidis, P., Bellanova, P., Costa, P. J. M., Finkler, C., Hadler, H., Koster, B., Lario, J., Reinhardt, E., Mathes-Schmidt, M., Ntageretzis, K., Pantosti, D., Papanikolaou, I., Sansò, P., Scicchitano, G., Smedile, A., Szczuciński, W. (2018): Publicity waves based on manipulated geoscientific data suggesting climatic trigger for majority of tsunami findings in the Mediterranean – Response to 'Tsunamis in the geological record: Making waves with a cautionary tale from the Mediterranean' by Marriner et al. (2017). – Z. Geomorphol. N. F. Suppl. Issue, http://www.ingentaconnect.com/content/schweiz/zfgs/pre-prints/content-zfg_suppl_00_0_0000_0000_voett_0547_prepub.

Addresses of the authors:

Margret Mathes-Schmidt (corresponding author) and Klaus Reicherter, Institude of Neotectonics and Natural Hazards, RWTH Aachen University, Lochnerstrasse 4–20, 52056 Aachen, Germany, email: m.mathes@nug.rwth-aachen.de

Ioannis Papanikolaou, Laboratory Mineralogy – Geology, Section of Geological Sciences, Department of Natural Resources Development and Agricultural Engineering, Agricultural University of Athens, 75 Iera Odos Str., 118 55 Athens, Greece, email: i.pap@aua.gr

Aggelos Pallikarakis, Department of Natural Resources Management and Agricultural Engineering, Agricultural University of Athens, 75 Iera Odos Str., 118 55 Athens, Greece, email: agpall@aua.gr

Manuscript received: 25 February 2019
Revisions requested: 19 March 2019
Revised version received: 8 May 2019
Accepted: 8 May 2019